Observations of the Antarctic ozone hole from 2003 - 2009

Braathen, G., World Meteorological Organization, Geneva, Switzerland; Van der A, R., Royal Netherlands Meteorological Institute, De Bilt, Netherlands; Anastou, A., Alfred Wegener Institute, Potsdam, Germany;
Bernhard, G., Biospherical Inc., San Diego, CA, USA; Campos, J., Dirección Meteorológica de Chile, Santiago, Chile; Chipperfield, M., University of Leeds, Leeds, UK; Ciattaglia, L., Consiglio Nazionale delle Ricerche, Rome, Italy;
Deshler, T., University of Wyoming, Laramie, WY, USA; Evans, R., National Oceanic and Atmospheric Administration, Boulder, CO, USA; Feng, W., University of Leeds, Leeds, UK; Fioletov, V., Environment Canada, Downsview, Ontario, Canada;
Garcia, R., Dirección Nacional de Meteorología, Montevideo, Uruguay; von der Gathen, P., Alfred Wegener Institute, Potsdam, Germany; Gelman, M., National Oceanic and Atmospheric Administration, Camp Springs, MD, USA;
Ginzburg, M., Servicio Meteorológico Nacional, Buenos Aires, Argentinal; Goutail, F., Centre National de la Recherche Scientifique, Verrières-le-Buisson, France; Hertzog, A., Laboratoire de Météorologie Dynamique, Palaiseau, France;
Johnson, B., National Oceanic and Atmospheric Administration, Boulder, CO, USA; Klekociuk, A., Australian Antarctic Division, Kingston, Tasmania, Australia; König-Langlo, G., Alfred Wegener Institute, Potsdam, Germany;
Long, C., National Oceanic and Atmospheric Administration, Camp Springs, MD, USA; Loyola, D., German Aerospace Center, Oberpfaffenhofen, Germany; Manney, G., Jet Propulsion Laboratory, Pasadena, CA, USA;
Marchand, M., Centre National de la Recherche Scientifique, Paris, France; McKenzie, R., National Institute for Water and Atmospheric Research, Lauder, New Zealand; McPeters, R., National Aeronautics and Space Administration, Greenbelt, MD, USA;
Mercer, J., University of Wyoming, Laramie, WY, USA; Nash, E., National Aeronautics and Space Administration, Greenbelt, MD, USA; Newman, P., National Aeronautics and Space Administration, Greenbelt, MD, USA;
Nichol, S., National Institute for Water and Atmospheric Research, Lauder, New Zealand; Ocampo, M., Dirección Nacional de Meteorología, Montevideo, Uruguay; Oltmans, S., National Oceanic and Atmospheric Administration, Boulder, CO, USA;
Pazmiño, A., Centre National de la Recherche Scientifique, Verrières-le-Buisson, France; Redondas, A., Instituto Nacional de Meteorología, Santa Cruz, Spain; Richter, A., University of Bremen, Bremen, Germany;
Rudolph, C., Alfred Wegener Institute, Potsdam, Germany; Shanklin, J., British Antarctic Survey, Cambridge, UK; Shudo, Y., Japanese Meteorological Agency, Tokyo, Japan; Vik, A.F., Norwegian Institute for Air Research, Kjeller, Norway;
Weber, M., University of Bremen, Bremen, Germany; Yela, M., Instituto Nacional de Técnica Aerospacial, Madrid, Spain; Zheng, X-D., Chinese Academy of Meteorological Sciences, Beijing, China.

World Meteorological Organization
Weather • Climate • Water

Meteorology

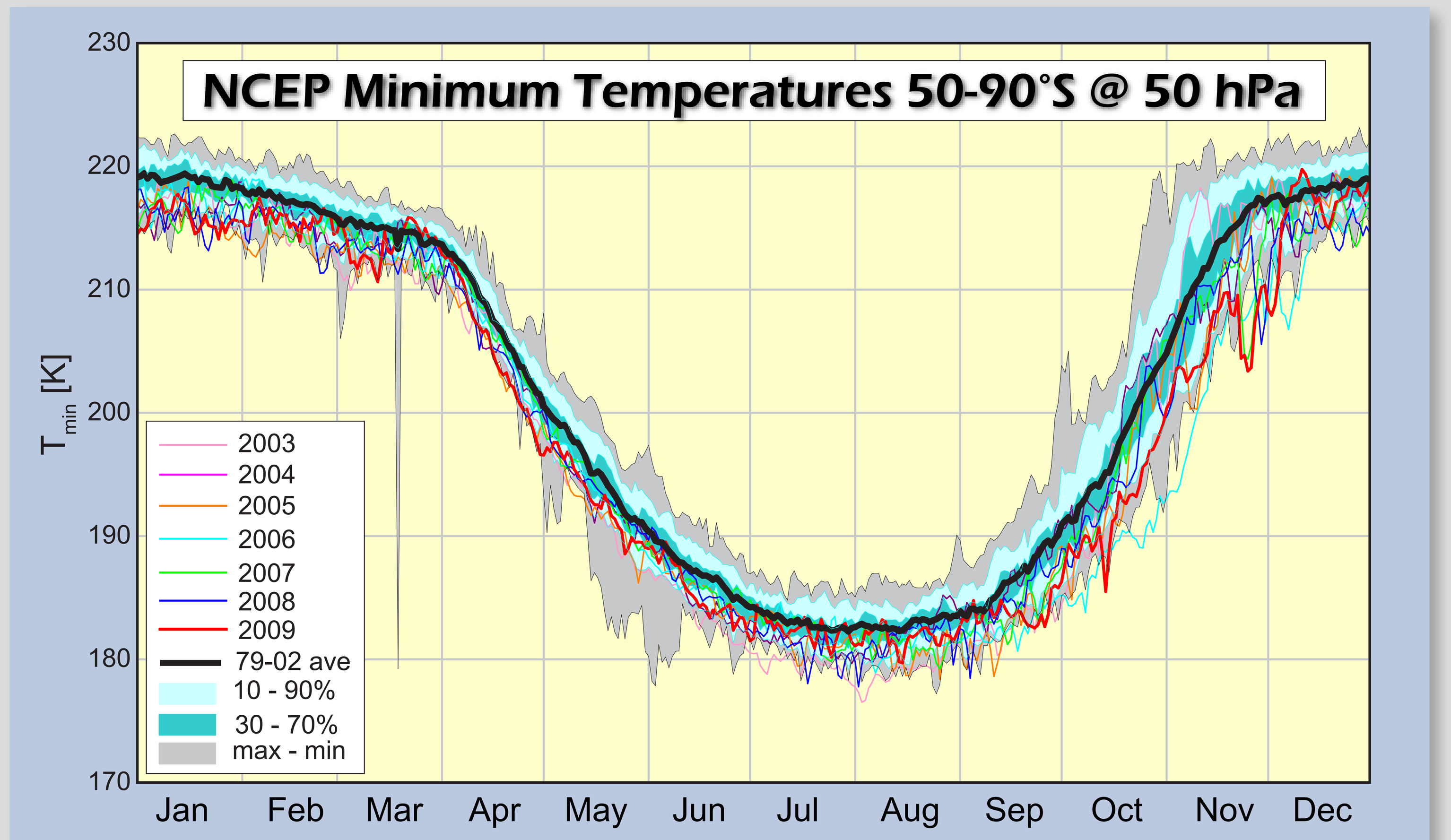

Figure 1. Time series of daily minimum temperatures at the 50 hPa isobaric level south of 50°S. The grey shaded area represents the highest and lowest daily minimum temperatures in the 1979-2002 time period. The light blue-green shaded area represents the 10th and 90th percentile values and the dark blue-green shaded area the 30th and 70th percentiles. The two horizontal green lines at 195 and 188 K show the thresholds for formation of PSCs of type I and type II, respectively. The plot is made with NCEP data downloaded from the Ozonewatch web site at NASA. It can be seen from the figure that 2003 was cold early in the season and 2006 was cold late in the season.

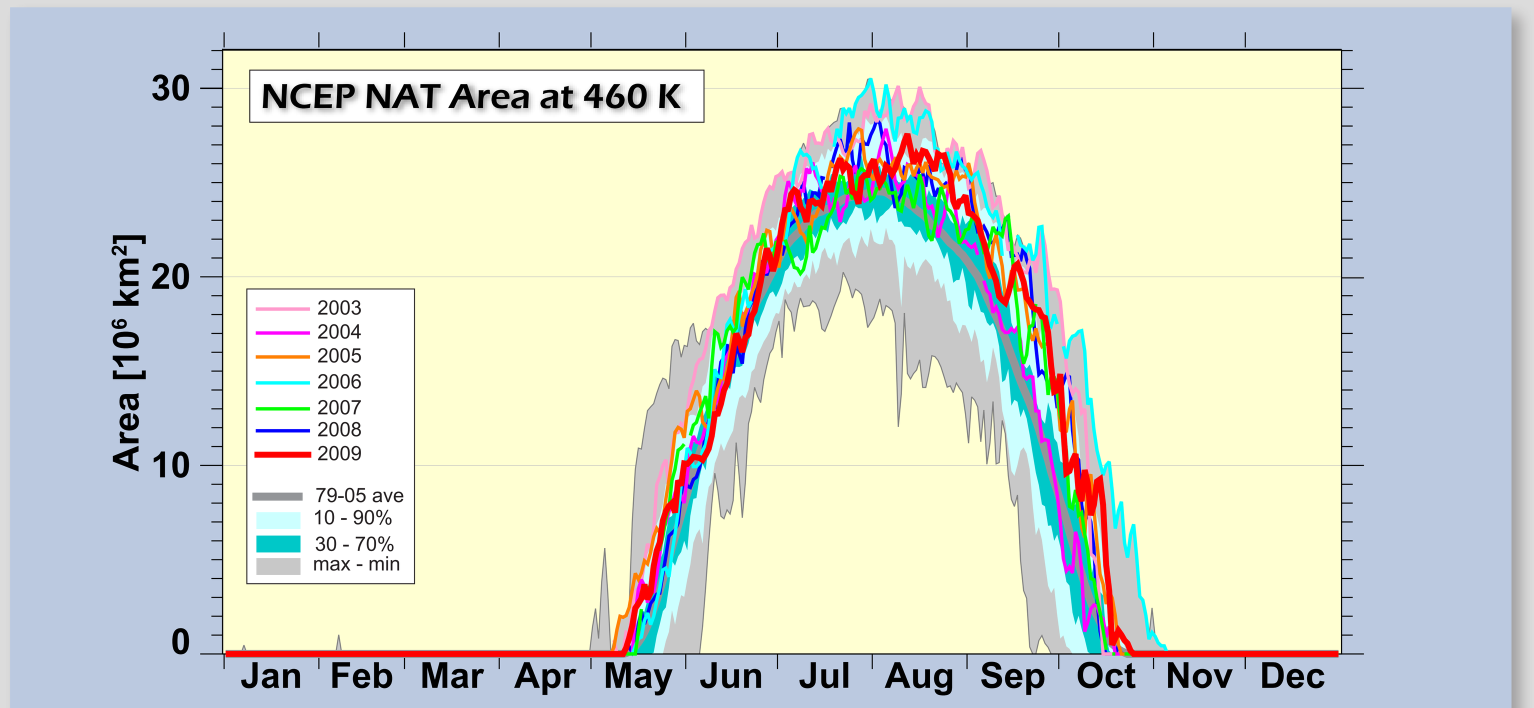

Figure 2. Time series of the area where temperatures are low enough for the formation of PSCs of type I at the 460 K isentropic level. This isentropic level corresponds to an altitude of approximately 18 km. The thick red curve shows 2009. The blue, green, cyan, orange, violet and pink curves represent 2008, 2007, 2006, 2005, 2004 and 2003, respectively. The average of the 1979-2005 period is shown for comparison in black. The grey shaded area represents the largest and smallest daily PSC areas in the 1979-2005 time period. The light blue-green shaded area represents the 10th and 90th percentile values and the dark blue-green shaded area the 30th and 70th percentiles. The plot is based on data from NOAA's Climate Prediction Center. It can be seen from the figure that the PSC area just reached the highest ever for the 1979-2005 time period in early August 2006 and that it was significantly higher than for any other year of this time period on most days in late September and October.

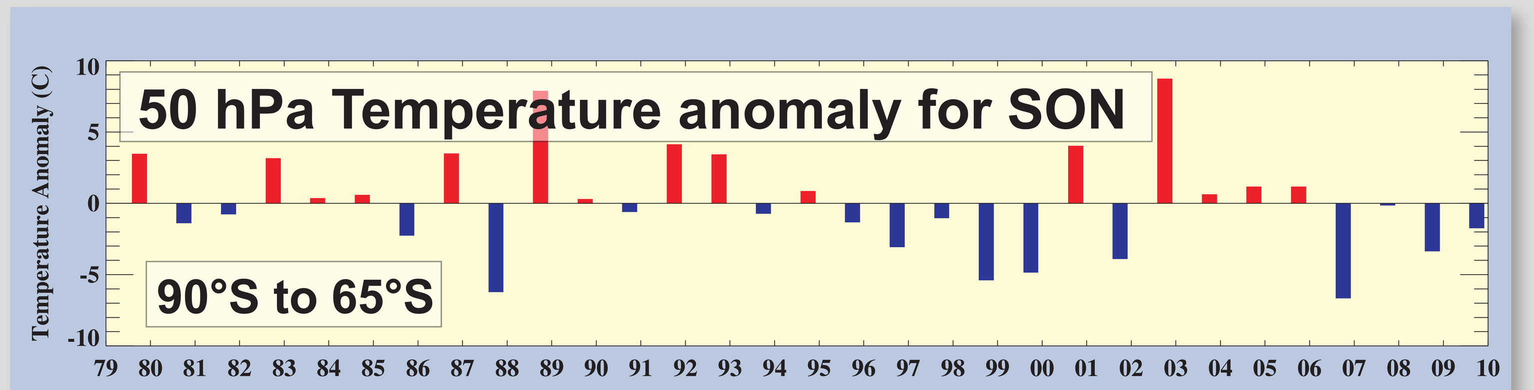

Figure 3. Temperature anomaly at the 50 hPa isobaric level for the region south of 65°S. Anomalies are deviations of monthly mean temperatures from the long-term (1979-2005) average for each month. Temperatures are from NOAA's Climate Prediction Center. One can see a cooling trend since the mid-1990s, and this trend is strengthened by the low temperatures in the 2006 and 2008 south polar vortex. Also 2009 was colder than the long-term average.

Ground-based observations

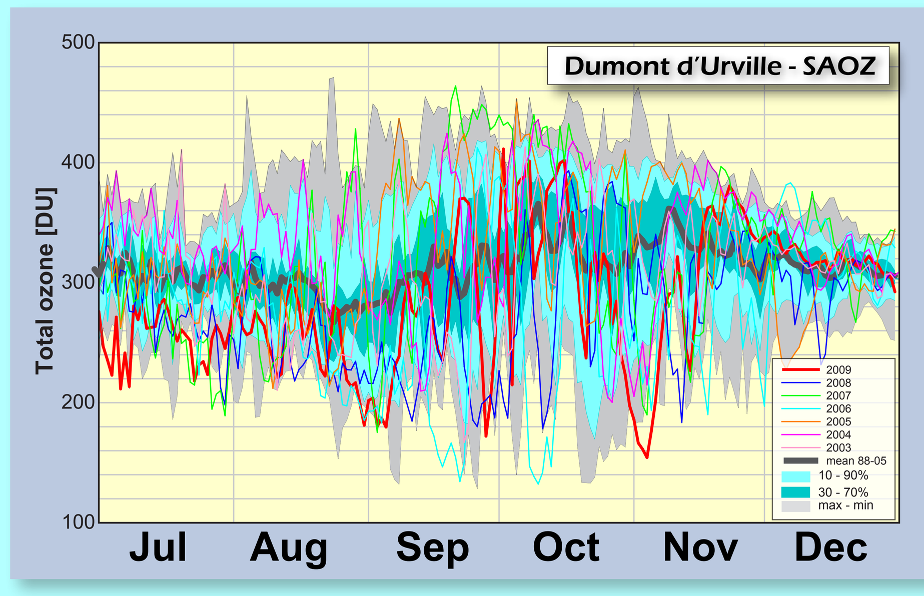

Figure 4. Time series of total ozone measurements from the French NDACC-GAW station Dumont d'Urville (66.7°S, 140.0°E). The thick grey curve shows the 1988-2005 average. The light blue shaded area shows the extreme values for each day during the 1988-2005 period. The SAOZ data are daily means calculated as the average of measurements taken at sunrise and sunset. Mid-winter, when sunrise and sunset happen at almost the same time, the sunrise and sunset values are almost identical. Later in the season, when there are several hours between sunrise and sunset, these two values can differ significantly, in particular on days when the vortex edge passes over the station. It can be seen from the figure that in late September and mid October 2006 record low values of total ozone were observed at this station.

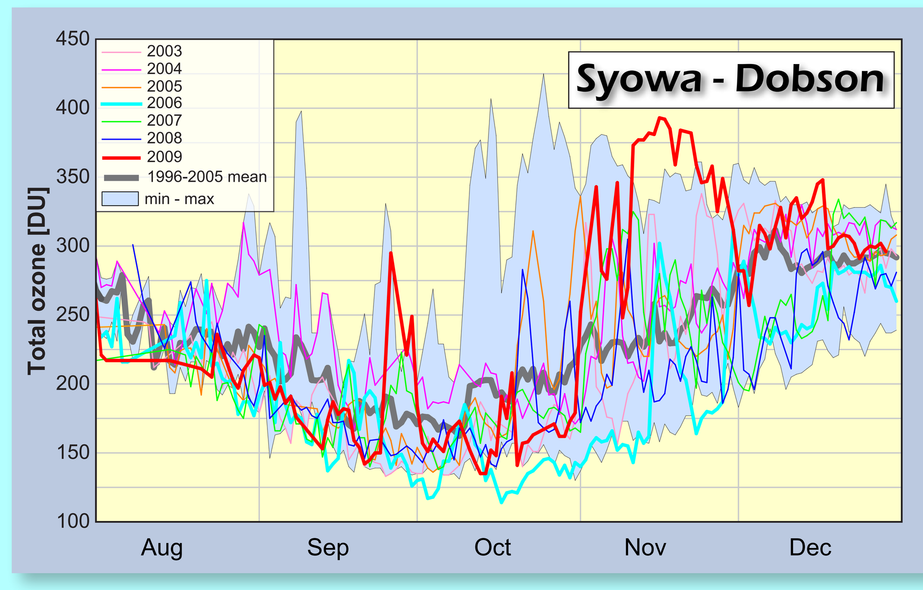

Figure 5. Time series of total ozone observations from the Japanese GAW station Syowa (69.0°S, 39.6°E). The coloured lines represent the years from 2003 to 2009. The thick grey line is the 1996-2005 average. The light blue shaded region shows the range of values for each day over the same time period. An all-time low total ozone column of 118 DU was measured on 4 October 2006. About two weeks later, on 17 October 2006, an even lower value of 114 DU was observed. These values are the lowest total ozone columns ever measured at Syowa since the measurements started in 1961.

Satellite observations

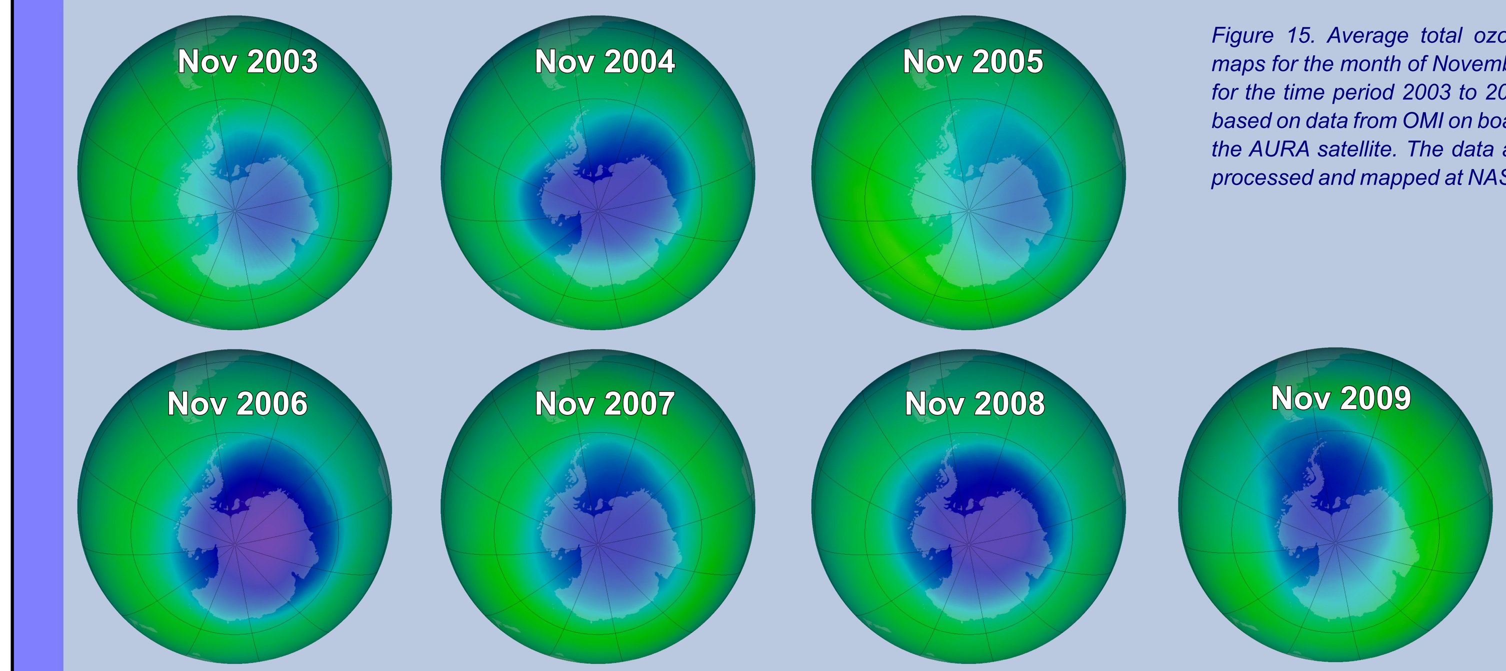

Figure 15. Average total ozone maps for the month of November for the time period 2003 to 2009 based on data from OMI on board the AURA satellite. The data are processed and mapped at NASA.

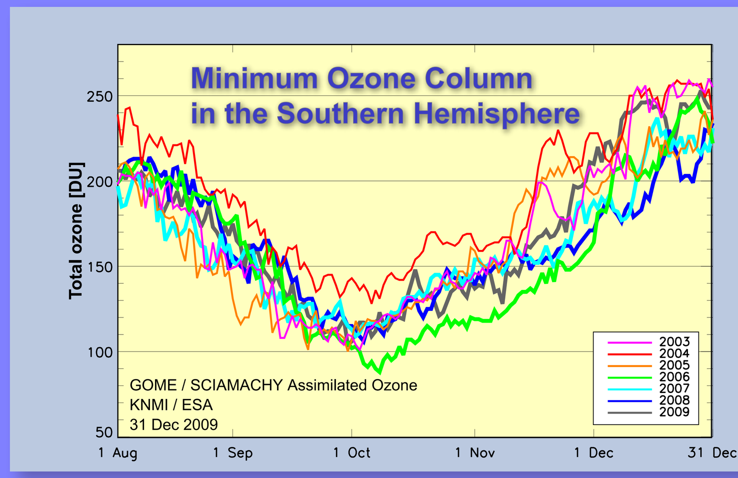

Figure 8. Daily minimum total ozone columns in the Southern Hemisphere as observed by GOME and SCIAMACHY from 2003 to 2009. The plot is provided by the Netherlands Meteorological Institute (KNMI).

Ozonesonde observations

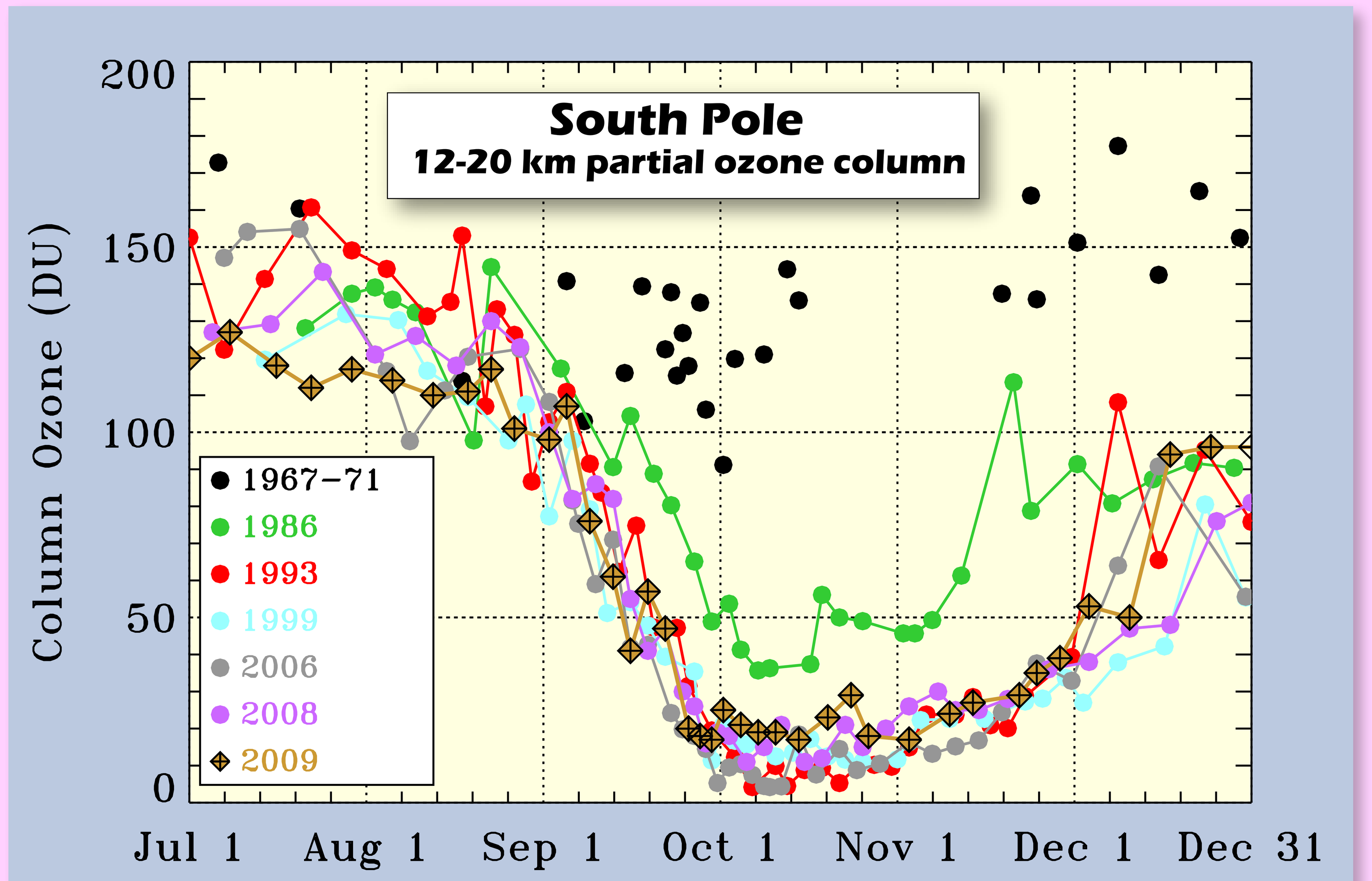

Figure 6. Ozonesonde observations from the NOAA-operated NDACC-GAW Amundsen-Scott station at the South Pole. Partial ozone columns for the altitude range 12-20 km are shown. Data for the last two ozone hole seasons are shown together with some other characteristic years. The black dots are from the period 1967-71, before the appearance of the first ozone hole. 1986 was the first year of continuous soundings at the South Pole. In 1993 one observed a record deep ozone hole related in part to the eruption of Mt. Pinatubo, particles from which augmented polar stratospheric clouds in the lower stratosphere. Ozone was nearly totally destroyed in the 12-20 km region through much of October of 1993. In 2006 one observed the most severe ozone hole so far.

Ozone hole statistics

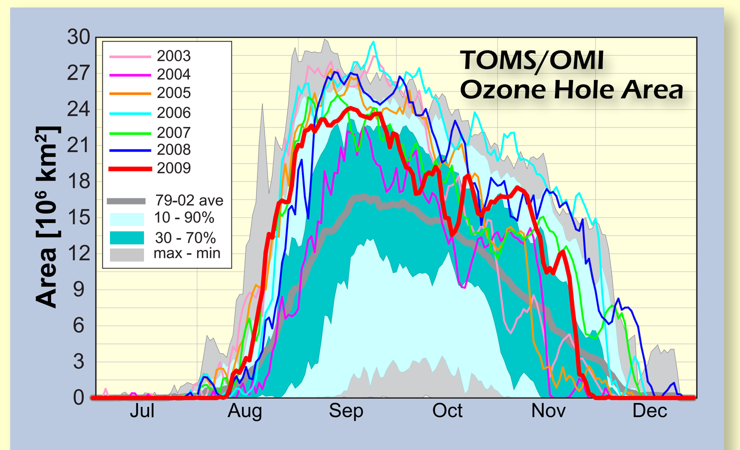

Figure 8. Area (millions of km²) where the total ozone column is less than 220 Dobson units. The smooth grey line is the 1979-2002 average. The dark green-blue shaded area represents the 30th to 70th percentiles and the light green-blue shaded area represents the 10th to 90th percentiles for the time period 1979-2002. The plot is based on data from the OMI instrument on the AURA satellite and provided by NASA.

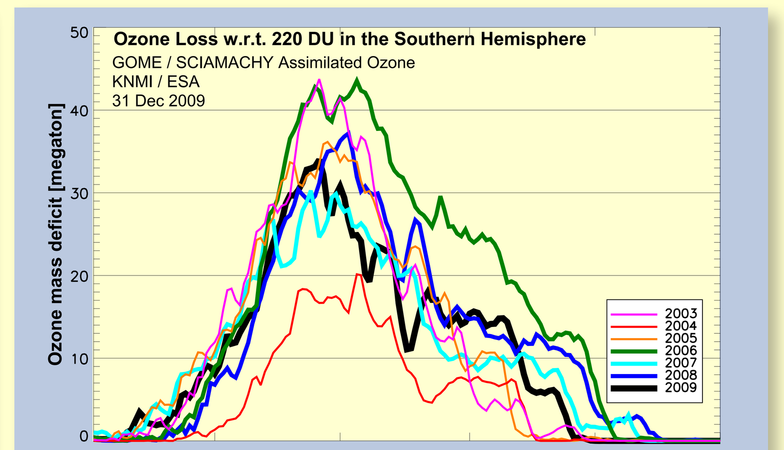

Figure 9. Ozone mass deficit for the years from 2003 to 2009. The mass deficit is the amount of ozone that would have to be added to the ozone hole in order to bring the total column up to 220 DU in those regions where the total column is below this threshold. This plot is produced by KNMI and is based on data from the GOME and SCIAMACHY satellite instruments.

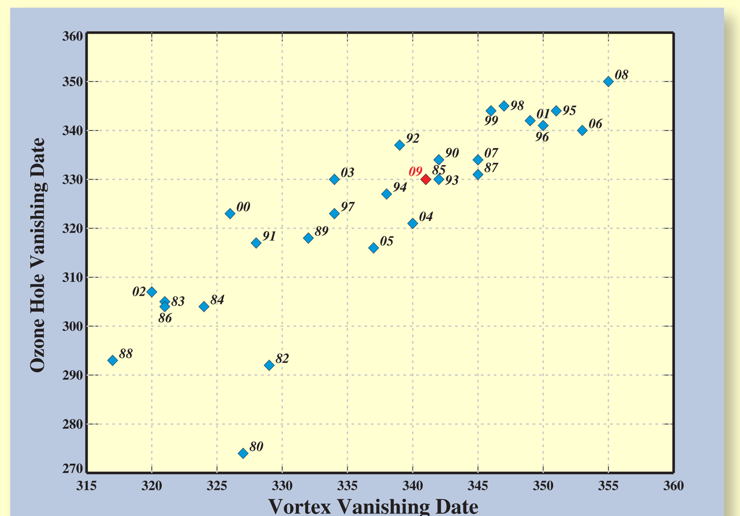

Figure 10. The figure illustrates the direct relationship between the persistence of the Antarctic ozone hole and the persistence of the SH polar vortex. In years when the winter polar vortex persisted later into the season, the duration of the ozone hole also tended to be extended. For the year 2008, the persistence of the SH polar vortex in the lower stratosphere extended longer than any previous year back to 1979. The persistence of the ozone hole, also to the middle of December, was also the longest on record. The ozone hole of 2009 was average in this regard.

Figure 11. Average area of the ozone hole for four different time periods based on observations fromTOMS and OMI. The upper left panel is for the last ten days of September, a period when the ozone hole usually is at its largest. The lower left panel is for the period 7 September - 13 October, which covers the period of both largest area and most severe mass deficit. Since the date of the peak area can vary from one year to another it also makes sense to look at the period of 30 consecutive days that gives the largest average ozone hole area. This is shown in the upper right panel. Finally, one can also look at the entire ozone hole season from before the onset of ozone depletion until the ozone hole is virtually dissolved. The period chosen is from 19 July to 1 December, and this is shown in the lower right panel. Data for these plots were provided by KNMI.